Research Article

EASL EUROPEAN ASSOCIATION FOR THE STUDY OF THE LIVER | JOURNAL OF HEPATOLOGY

Galectin-3 ablation protects mice from diet-induced NASH: A major scavenging role for galectin-3 in liver

Carla Iacobini[1,†], Stefano Menini[1,†], Carlo Ricci[1,†], Claudia Blasetti Fantauzzi[1], Angela Scipioni[1], Laura Salvi[1], Samantha Cordone[1], Francesca Delucchi[1], Matteo Serino[2], Massimo Federici[2], Flavia Pricci[3], Giuseppe Pugliese[1,*]

[1]*Department of Clinical and Molecular Medicine, "La Sapienza" University, Rome, Italy;* [2]*Department of Internal Medicine, "TorVergata" University, Rome, Italy;* [3]*Department of Cell Biology and Neurosciences, National Institute of Health of Italy, Rome, Italy*

Background & Aims: Excess fatty acid oxidation and generation of reactive carbonyls with formation of advanced lipoxidation endproducts (ALEs) is involved in nonalcoholic steatohepatitis (NASH) by triggering inflammation, hepatocyte injury, and fibrosis. This study aimed at verifying the hypothesis that ablation of the ALE-receptor galectin-3 prevents experimental NASH by reducing receptor-mediated ALE clearance and downstream events.

Methods: Galectin-3-deficient (*Lgals3*$^{-/-}$) and wild type (*Lgals3*$^{+/+}$) mice received an atherogenic diet or standard chow for 8 months. Liver tissue was analyzed for morphology, inflammation, cell and matrix turnover, lipid metabolism, ALEs, and ALE-receptors.

Results: Steatosis was significantly less pronounced in *Lgals3*$^{-/-}$ than *Lgals3*$^{+/+}$ animals on atherogenic diet. NASH, invariably detected in *Lgals3*$^{+/+}$ mice, was observed, to a lower extent, only in 3/8 *Lgals3*$^{-/-}$ mice, showing less inflammatory, degenerative, and fibrotic phenomena than *Lgals3*$^{+/+}$ mice. This was associated with higher circulating ALE levels and lower tissue ALE accumulation and expression of other ALE-receptors. Up-regulation of hepatic fatty acid synthesis and oxidation, inflammatory cell infiltration, pro-inflammatory cytokines, endoplasmic reticulum stress, hepatocyte apoptosis, myofibroblast transdifferentiation, and impaired Akt phosphorylation were also significantly attenuated in *Lgals3*$^{-/-}$ animals. Galectin-3 silencing in liver endothelial cells resulted in reduced N^{ε}-carboxymethyllysine-modified albumin uptake and ALE-receptor expression.

Conclusions: Galectin-3 ablation protects from diet-induced NASH by decreasing hepatic ALE accumulation, with attenuation of inflammation, hepatocyte injury, and fibrosis. It also reduced up-regulation of lipid synthesis and oxidation causing less fat deposition, oxidative stress, and possibly insulin resistance. These data suggest that galectin-3 is a major receptor involved in ALE uptake by the liver.

Keywords: Steatosis; Inflammation; Fibrosis; Advanced lipoxidation endproducts; Oxidative stress.

Received 28 December 2009; received in revised form 8 September 2010; accepted 14 September 2010; available online 29 October 2010

* Corresponding author. Address: Department of Clinical and Molecular Medicine, "La Sapienza" University of Rome, via di Grottarossa 1035-1039 Rome, Italy. Tel.: +39 0633775049; fax: +39 0633775001.

E-mail address: giuseppe.pugliese@uniroma1.it (G. Pugliese).

† These contributed equally to this work.

Introduction

Non-alcoholic fatty liver disease (NAFLD) encompasses various disease conditions, from simple steatosis to nonalcoholic steatohepatitis (NASH), cirrhosis, and possibly hepatocellular carcinoma [1]. It is associated with insulin resistance and the metabolic syndrome [2], which causes fat accumulation within the liver via increased fatty acid (FA) delivery from adipose tissue and enhanced hepatic FA import and synthesis exceeding the rate of FA export and catabolism [3].

Based on the "two hits" hypothesis, transition from steatosis to NASH is dependent on the superimposition of oxidative phenomena ("second hit") on top of fat accumulation ("first hit"), which sensitizes the liver to oxidant-dependent injury resulting in tissue inflammation and hepatocyte degeneration [4]. More recently, it has been suggested that FA metabolism itself may be responsible for this transition [5], via induction of endoplasmic reticulum (ER) stress and increased production of reactive oxygen species (ROS) by mitochondrial β-oxidation and, when its capacity becomes overwhelmed, also by peroxisomal β-oxidation and endoplasmic reticulum ω-oxidation of FAs [4]. In turn, ROS would trigger the self-reinforcing inhibitor κB kinase-β/nuclear factor κB (NFκB)/tumour necrosis factor-α (TNF)-α cycle [6], which initiates and maintains a T helper 1 (Th1)- and macrophage 1 (M1)-mediated inflammatory response [7]. Further progression to cirrhosis may require a "third hit", which specifically promotes fibrosis by inducing myofibroblast transdifferentiation of hepatic stellate cells (HSCs), a step involving a shift of the innate immune system toward a Th2- and M2-phenotype [7].

ROS also peroxidize unsaturated lipids generating endoperoxides, which are further metabolized to reactive carbonyl species (RCS), such as 4-hydroxy-2-nonenal (HNE) and glyoxal. RCS and the advanced lipoxidation endproduct (ALE) adducts or cross-links, generated by their reaction with proteins [8], are more persistent than ROS, thus causing more inflammation and injury and also direct activation of fibrogenesis [9].

The liver is the main catabolic site for ALEs and advanced glycation endproducts (AGEs), as indicated by the findings that plasma

ALE/AGE levels increase markedly in patients with liver cirrhosis, correlate with disease severity and inversely with residual liver function, and decrease after liver transplantation [10]. Tracer studies indicated that BSA-AGE injected into rats is mainly eliminated by sinusoidal liver cells, particularly endothelial more than Kupffer cells [11]. AGE-BSA undergoes receptor-mediated endocytosis [11] and subsequent degradation by detoxifying enzymes [8].

Progressive fat accumulation results in increased ALE formation and receptor-mediated endocytosis, which triggers signalling pathways leading to a chronic low-grade inflammatory setting which may drive the development of NASH [12]. It also causes impaired scavenging function of liver cells [13], thus hampering hepatic removal of ALEs/AGEs and favouring their deposition in various extra-hepatic organs, including vessels, which might explain the increased cardiovascular risk of patients suffering from NAFLD/NASH [14].

ALEs/AGEs are recognized by the pattern recognition receptors of innate immunity [15], which include the scavenger receptors (SRs), the toll-like receptors (TLRs), and the classical AGE receptors. Peritoneal macrophages from SR-A knockout and SR-A/CD36 double knockout mice showed reduced uptake and degradation of AGE-BSA and/or modified LDLs, as compared with wild-type macrophages [16,17], thus suggesting a major role for these receptors in AGE/ALE endocytosis. However, endocytic uptake of AGEs by liver endothelial cells (LECs) was shown to be mediated by a receptor distinct from SR-A [16] and CD36 [18], but with closely similar ligand specificity. Receptor for AGEs (RAGE) is found predominantly in hepatocytes, whereas galectin-3 is highly expressed in Kupffer cells, and the levels of both receptors were reported to increase with the extent of liver damage [19]. RAGE blockade was shown to inhibit experimental hepatic fibrosis [20], whereas it was found to be up-regulated during HSC myofibroblast transdifferentiation [21]. Deletion of galectin-3 gene was shown to block myofibroblast activation and matrix production both *in vitro* and *in vivo* [22], though other investigators have reported that mice with galectin-3 disruption develop NAFLD/NASH spontaneously with aging [23].

We previously showed that galectin-3 ablation accelerates atherosclerosis and renal disease induced by an atherogenic diet and that this is associated with increased circulating and tissue ALE/AGE levels [24,25]. Since this diet is known to induce NASH [4], we verified whether, in these mice, deletion of galectin-3 accelerates NASH, as in other ALE-related disease conditions, or rather prevents the development of liver disease by impairing hepatic ALE uptake, thus reducing ALE-induced tissue injury. A corollary of the latter hypothesis is that galectin-3 plays a major role in the removal of circulating ALEs/AGEs by the liver.

Materials and methods

Design

Adult (aged 3 months) female galectin-3 knockout (*Lgals3*$^{-/-}$) and coeval C57BL/6 wild type (*Lgals3*$^{+/+}$) mice were fed for 8 months with a Paigen's atherogenic high-fat diet (HFD, Mucedola, Settimo Milanese, Italy), containing 15% fat, 1.25% cholesterol, and 0.5% Na-cholate, or a standard normal-fat diet (NFD, Charles River Italia, Calco, Italy), containing 4% fat [24,25]. This study was approved by the local Ethics Committee. The animals were housed and cared for in accordance with the "Principles of Laboratory Animal Care" (NIH Publication no. 85–23, revised 1985) and received water and food at libitum. At the end of the 8-month period, the animals were anesthetized with intraperitoneal ketamine (Imalgene®, 60 mg/kg body weight) and xylazine (Rompum®, 7.5 mg/kg body weight); a blood sample was obtained and the liver was removed. Eight animals per group were examined for liver pathology. Additional mice were injected with 5 IU insulin (Actrapid@, Novo Nordisk, Copenhagen, DK) or vehicle 5 min prior to sacrifice, then the liver and quadricep muscles were sampled. To assess the role of galectin-3 in ALE/AGE liver uptake, human LECs were plated onto fibronectin-coated dishes and cultured in Endothelial Cell Medium supplemented with 5% FBS, antibiotics, and Endothelial Cell Growth Supplement (ScienceCell Research Laboratories, Carlsbad, CA, USA), at 37 °C in 95% air-5% CO_2 humidified atmosphere. Then, galectin-3 was silenced using Lipofectamine RNAiMAX (Invitrogen, Carlsbad, CA, USA) and Silencer Select Pre-designed siRNA (S8149, Ambion, Austin, TX, USA), according to the manufacturer's instructions. After 48 h, LECs were probed with 5–50 μg/ml N^{ε}-carboxymethyllysine (CML)-modified human serum albumin (HSA), prepared as previously described [26].

Liver morphology/morphometry

Liver morphology was assessed based on the American Association for the Study of Liver Disease Guidelines [27]. In hematoxylin and eosin-stained sections, steatosis grading was assessed based on the percentage of parenchyma involved (grades 0 to 3 as follows: 0, no fat; 1, <33%; 2, 33–66%; 3, >66%). The steatosis grade and the presence of inflammation, hepatocyte degeneration (acidophil or Councilman's bodies, ballooning and Mallory's hyaline), and fibrosis were then considered for NAFLD staging. Subsequently, samples from NAFLD stage 3 and 4 mice (i.e. NASH) were graded based on the type of fat (macrovesicular, microvesicular, or mixed), and the extent of inflammation (scored 0 to 3 as follows: 0, no inflammation; 1, mild; 2, moderate; 3, severe), and hepatocyte degeneration or necrosis. Finally, sections stained with Masson's trichrome were staged for NASH by assessing the extent and distribution of fibrosis.

Biochemistry

Blood glucose was measured with the aid of an automated colorimetric instrument (Glucocard G meter®, Menarini, Florence, Italy), free FAs using the NEFA C kit (Wako, Osaka, Japan), and serum cholesterol, triglycerides, aspartate transaminase (AST), and alanine transaminase (ALT) by standard chemical methods (VITROS 5, 1 FS Chemistry System, Ortho-Clinical Diagnostics, Rochester, NY).

ELISA

Serum ALE/AGE levels were assessed by a competitive ELISA technique, using a mouse monoclonal antibody recognizing also CML which, under these conditions, originates primarily from lipoxidation-derived glyoxal [24,25]. The activation of NFκB/p65 was assessed using the Mercury TransFactor kit (BD Biosciences Clontech, Palo Alto, CA) on nuclear protein liver extracts.

Immunohistochemistry and Western blot

Immunohistochemical analysis [24,25] was performed to assess the liver content and distribution of: (a) the markers of murine macrophage activation (F4/80), T lymphocytes (CD3), Th1/M1-mediated inflammatory response (CX chemokine receptor 3, CXCR3, and monocyte chemoattractant protein-1, MCP-1), HSC myofibroblast differentiation (α-smooth muscle actin, α-SMA), and apoptotic cells (active caspase-3); (b) the lipoxidation products HNE adducts and CML; and (c) the ALE/AGE-receptors CD36, RAGE, and galectin-3. Sections were analyzed using the Optimas 6.5 image analysis system. Total and phosphorylated Akt expression in liver and quadriceps muscle tissue from mice injected with insulin or vehicle and CML content in LEC monolayers (and conditioned media) probed with CML-HSA were assessed by Western blot analysis (see Supplemental Table 1 for primary antibodies used in these assays).

RT-PCR

The following transcripts were measured by competitive RT-PCR [24,25]: (a) the inflammatory mediators *CXCR3*, *MCP-1*, cycloxygenase-2 (*Cox-2*), *TNF-α*, interferon-γ (*IFN-γ*), and interleukin (*IL*)-*4*, *6*, and *10*; (b) the extracellular matrix proteins *fibronectin* and *collagen I*, and the pro-fibrotic cytokines transforming growth factor-β (*TGF-β*) and connective tissue growth factor (*CTGF*); (c) the transcription factors regulating lipid metabolism, sterol regulatory element binding protein *(SREBP)-1c* and *2*, peroxisome proliferator-activated receptor *(PPAR)-α*

Table 1. Metabolic parameters. Body weight, blood glucose, cholesterol, triglycerides, free FAs, ALT, ALT, and ALEs/AGEs in NFD- and HFD-fed *Lgals3*$^{+/+}$ and *Lgals3*$^{-/-}$ mice (mean ± SD; $n = 8$ per group, except $n = 5$ for free FAs, AST, and ALT). $*p < 0.001$ vs. NFD-fed mice; $^{\dagger}p < 0.001$ or $^{\ddagger}p < 0.01$ vs. *Lgals3*$^{+/+}$ mice.

	Lgals3$^{+/+}$-NFD	*Lgals3*$^{-/-}$-NFD	*Lgals3*$^{+/+}$-HFD	*Lgals3*$^{-/-}$-HFD
Body weight (g)	26.98 ± 0.91	26.09 ± 1.52	26.93 ± 1.21	25.83 ± 1.12
Blood glucose (mg/dl)	111.38 ± 5.42	110.75 ± 7.52	117.00 ± 7.67	116.25 ± 7.21
Cholesterol (mg/dl)	61.25 ± 8.53	61.13 ± 6.51	221.75 ± 16.18*	219.75 ± 27.19*
Triglycerides (mg/dl)	74.88 ± 14.78	75.38 ± 8.77	243.13 ± 16.09*	249.63 ± 26.14*
Free FAs (mEq/L)	0.33 ± 0.08	0.32 ± 0.10	0.42 ± 0.11	0.38 ± 0.10
AST (IU/L)	36.40 ± 5.03	35.60 ± 4.62	88.40 ± 15.65*	56.20 ± 9.88*‡
ALT (IU/L)	19.60 ± 4.56	18.00 ± 3.39	113.20 ± 14.24*	58.20 ± 8.07*†
ALEs/AGEs (U/ml)	3.12 ± 0.69	3.34 ± 0.87	7.68 ± 0.50*	11.75 ± 2.43*†

and γ, and liver X receptor *(LXR)*- α and *β*; (d) the enzymes of FA synthesis, acetyl-CoA carboxylase (*ACC*) and FA synthase (*FAS*), peroxisomal β-oxidation, acyl-CoA oxidase (*ACO*), ER ω-oxidation cytochrome P450-2E1 (*CYP2E1*), and cholesterol synthesis, hydroxymethylglutaryl *(HMG)-CoA* reductase; (e) the protein responsible for triglyceride transfer to apolipoprotein B100, microsomal triglyceride transfer protein (*MTTP*); (f) the regulator of ER stress-mediated apoptosis CCAAT/enhancer binding protein (C/EBP) homologous protein (*CHOP*); and (g) the ALE/AGE-receptors *SR-A1*, *CD36*, *TLR-2* and *4*, *RAGE*, and *galectin-3* (see Supplemental Table 2 for primers). Results were quantified by scanning densitometry using the ImageJ software and expressed as the ratio of each target to 18S rRNA level.

Statistical analysis

Results are expressed as mean ± SD. Statistical significance was evaluated by one-way ANOVA followed by the Student–Newman–Keuls test for multiple comparisons. A *p*-value <0.05 was considered significant. All statistical tests were performed on raw data.

Results

Metabolic parameters

Body weight and blood glucose levels did not differ among groups, whereas serum cholesterol and triglycerides increased significantly and while free FAs did not in HFD- vs. NFD-mice, with no difference between the two genotypes (Table 1). We previously reported that HFD-fed mice showed biochemical features of insulin resistance, including increased insulin and HOMA-IR, decreased adiponectin, and a blunted blood glucose surge and fall, respectively, in response to intraperitoneal glucose and the insulin tolerance test; changes vs. NFD-fed animals were significant only in *Lgals*$^{+/+}$ mice, though no difference was detected between HFD-fed *Lgals*$^{+/+}$ and *Lgals*$^{-/-}$ mice [24,25].

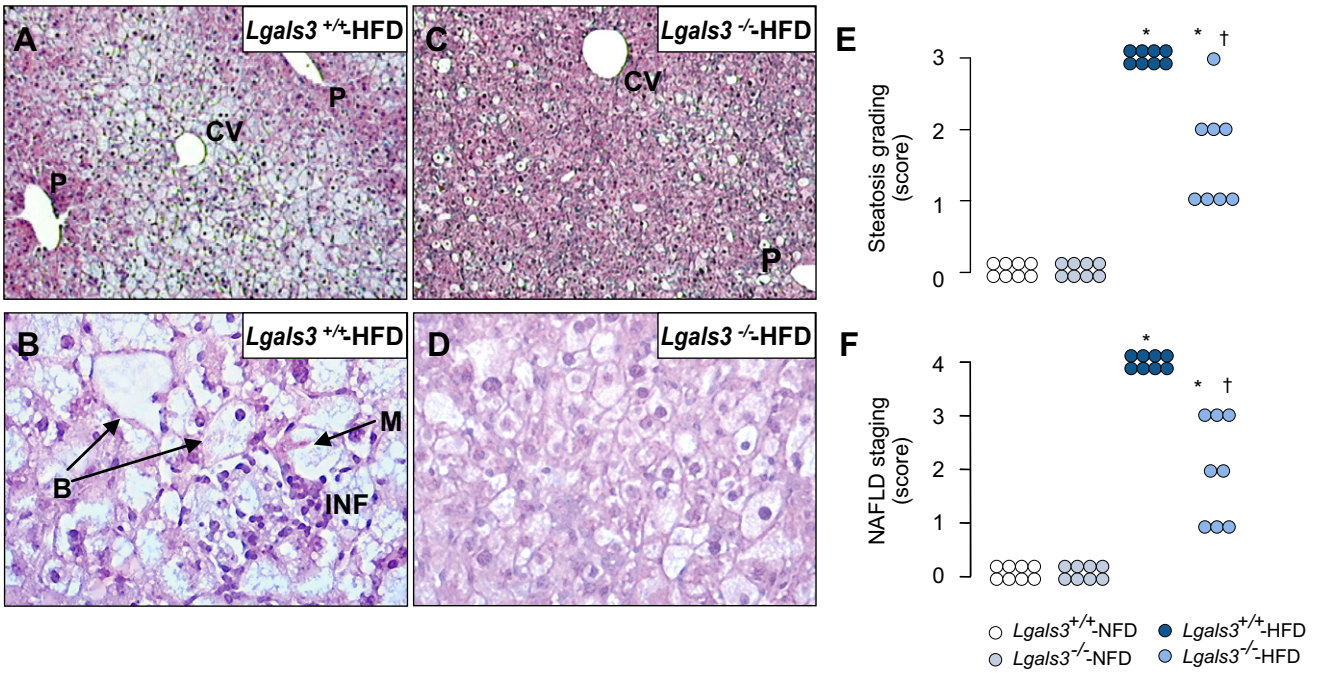

Fig. 1. NAFLD grading and staging. Liver sections from representative HFD-fed *Lgals3*$^{+/+}$ (A and B) and *Lgals3*$^{-/-}$ (C and D) mice stained with hematoxylin and eosin (original magnification A–C 100×, B–D 400×) and steatosis grading (E) and NAFLD staging (F) in NFD- and HFD-fed *Lgals3*$^{+/+}$ and *Lgals3*$^{-/-}$ mice (mean ± SD; $n = 8$ per group). *p* = portal area; CV = centrolobular vein; B = ballooning degeneration; M = Mallory's body; INF = inflammation. $*p < 0.001$ vs. NFD-fed mice; $^{\dagger}p < 0.001$ vs. *Lgals3*$^{+/+}$ mice.

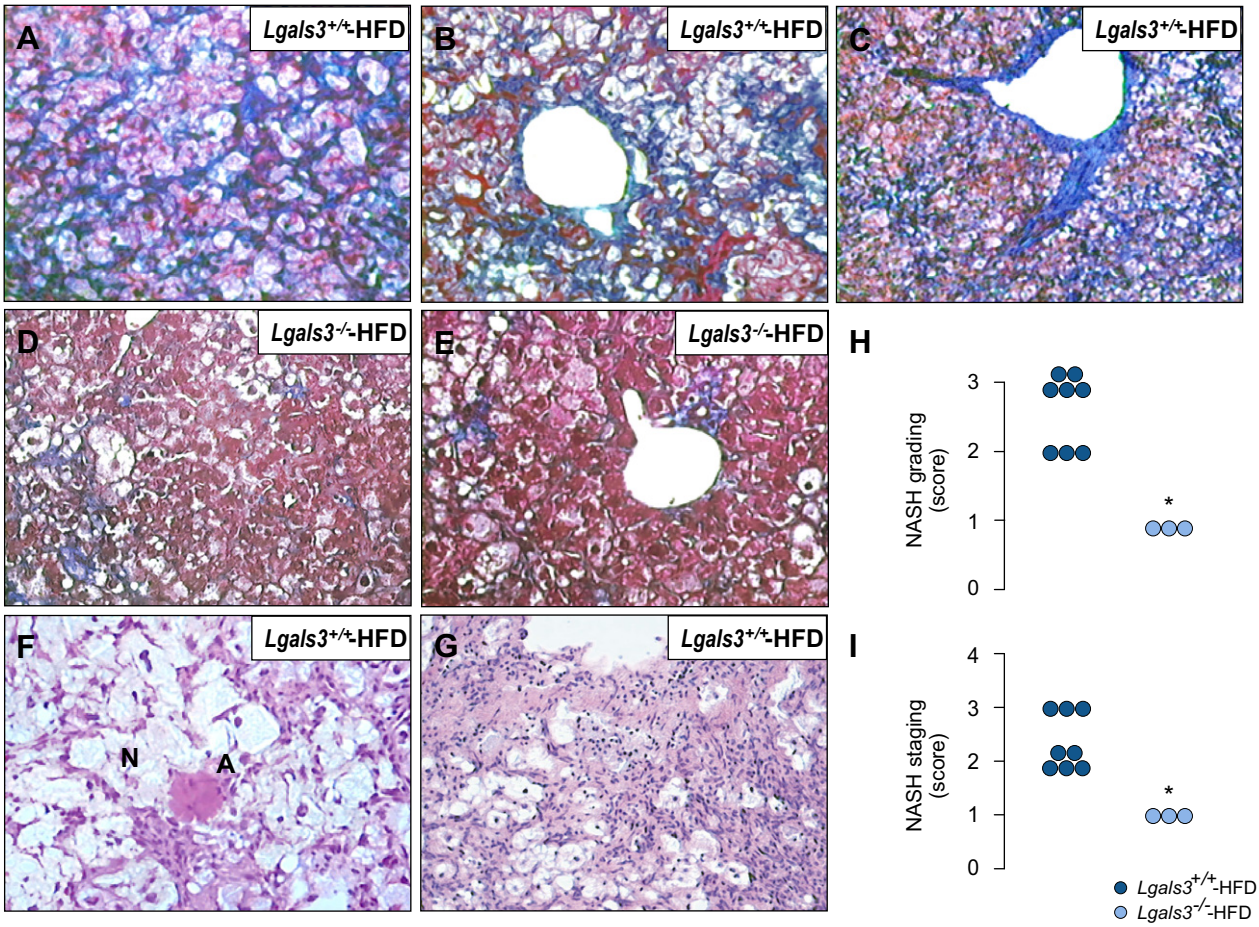

Fig. 2. NASH grading and staging. Liver sections from representative HFD-fed *Lgals3*$^{+/+}$ (A) perisinusoidal/pericellular fibrosis; (B) perivenular/centrolobular fibrosis; (C) bridging fibrosis; and *Lgals3*$^{-/-}$ (D–E) mild focal perisinusoidal/pericellular fibrosis with normal centrolobular vein in (E) mice stained with Masson's trichrome and from representative HFD-fed *Lgals3*$^{+/+}$ mice stained with hematoxylin and eosin (F) acidophil Councilman's body [A], focal necrosis [N], Kupffer cell activation, and perisinusoidal fibrosis; and *G*: portal inflammation with mononuclear cell infiltration and lobular inflammation with neutrophils around an area of hepatocyte degeneration) (original magnification 250×, except *C*, 100×, and F, 400×); and NASH grading (H) and staging (I) in the HFD-fed *Lgals3*$^{+/+}$ ($n = 8$) and *Lgals3*$^{-/-}$ ($n = 3$) mice fulfilling NASH criteria (mean ± SD). $^{*}p < 0.001$ vs. *Lgals3*$^{+/+}$ mice.

NAFLD

Steatosis was detected only in HFD-fed mice, but it was of higher grade in *Lgals3*$^{+/+}$ than in *Lgals3*$^{-/-}$ mice. While all *Lgals3*$^{+/+}$-HFD mice showed stage 4 NAFLD (macrovesicular steatosis, associated with portal and lobular inflammation, Councilman's bodies, ballooning degeneration, Mallory's hyaline, and fibrosis), only 3 *Lgals3*$^{-/-}$ animals fell into stage 3 (mixed steatosis with lobular inflammation and ballooning degeneration). The remaining *Lgals3*$^{-/-}$ mice did not fulfil NASH criteria, with 2 and 3 animals showing stage 2 (predominantly microvesicular steatosis with mild lobular inflammation) and 1 (simple steatosis) NAFLD, respectively (Fig. 1).

NASH

Of the *Lgals3*$^{+/+}$ animals fed a HFD, 3 showed grade 2 (moderate) and 5 grade 3 (severe or florid) NASH, whereas 5 exhibited stage 2 (zone 3 portal/periportal, perivenular/centrolobular, perisinusoidal/pericellular fibrosis; focal or extensive) and 3 stage 3 (bridging fibrosis, focal or extensive) fibrosis. The 3 *Lgals3*$^{-/-}$ mice fulfilling NASH criteria were graded 1 (mild) for NASH and staged 1 (i.e. as stage 2, except portal fibrosis) for fibrosis (Fig. 2).

Inflammatory cells and mediators

A more marked increase in monocyte–macrophage, lymphocyte, and CXCR3 and MCP-1 protein content was detected in *Lgals3*$^{+/+}$ vs. *Lgals3*$^{-/-}$ mice fed a HFD, especially in periportal areas (Supplemental Fig. 1A–L). The activation of NFκB/p65 and the gene expression levels of both Th1/M1 (*CXCR3*, *MCP-1*, *TNF-α*, *IL-6*, *IFN-γ*) and Th2/M2 (*IL-4* and *IL-10*) cytokines increased more markedly or exclusively in *Lgals3*$^{+/+}$ mice, as compared with *Lgals3*$^{-/-}$ animals (Table 2).

Liver cell and matrix turnover

The rate of apoptosis was negligible in NFD-fed mice and increased significantly only in *Lgals3*$^{+/+}$ mice fed a HFD (Fig. 3A–C). Upon HFD diet, gene expression of fibronectin and

Table 2. Inflammation, fibrosis, lipid metabolism, ER stress, and ALE/AGE-receptors. Liver NFκB/p65 activation and gene expression of *CXCR3*, *MCP-1*, Cox-2, *TNF-α*, *IFN-γ*, *IL-4*, 6, and *10*, *fibronectin*, *collagen I*, *TGF-β*, *CTGF*, *SREBP-1c* and *2*, *PPAR-α* and *γ*, *LXR-α* and *β*, *ACC*, *FAS*, *ACO*, *CYP2E1*, *HMG-CoA reductase*, *MTTP*, *CHOP*, *SR-A1*, *CD36*, *TLR-2* and *4*, *RAGE*, and *galectin-3* in NFD- and HFD-fed *Lgals3*$^{+/+}$ and *Lgals3*$^{-/-}$ mice (mean ± SD; $n = 4$ per group). $^{*}p$ <0.001 or $^{\dagger}p$ <0.05 vs. NFD-fed mice; $^{\ddagger}p$ <0.001, $^{\S}p$ <0.01 or $^{\#}p$ <0.05 vs. *Lgals3*$^{+/+}$ mice.

	Lgals3$^{+/+}$-NFD	*Lgals3*$^{-/-}$-NFD	*Lgals3*$^{+/+}$-HFD	*Lgals3*$^{-/-}$-HFD
NFκB/p65	0.15 ± 0.03	0.14 ± 0.02	0.73 ± 0.16*	0.29 ± 0.10
CXCR3	1.12 ± 0.36	1.14 ± 0.30	20.82 ± 3.81*	11.52 ± 3.83*‡
MCP-1	0.09 ± 0.03	0.08 ± 0.03	1.16 ± 0.07*	0.66 ± 0.06*‡
Cox-2	0.18 ± 0.08	0.19 ± 0.04	1.26 ± 0.18*	0.84 ± 0.18*‡
TNF-α	0.29 ± 0.15	0.18 ± 0.07	1.25 ± 0.19*	0.50 ± 0.05*‡
Il-6	0.72 ± 0.23	0.67 ± 0.08	2.71 ± 1.10*	0.88 ± 0.11‡
IFN-γ	0.23 ± 0.06	0.23 ± 0.06	1.03 ± 0.19*	0.33 ± 0.08‡
IL-4	0.92 ± 0.23	0.88 ± 0.19	2.13 ± 0.56*	0.97 ± 0.14‡
IL-10	0.25 ± 0.07	0.18 ± 0.04	0.67 ± 0.10*	0.45 ± 0.07*‡
fibronectin	1.22 ± 0.15	1.02 ± 0.16	1.89 ± 0.15*	1.30 ± 0.14‡
collagen I	0.45 ± 0.08	0.34 ± 0.13	1.03 ± 0.15*	0.76 ± 0.04*§
TGF-β	0.34 ± 0.08	0.26 ± 0.09	2.42 ± 0.57*	1.14 ± 0.13*‡
CTGF	1.09 ± 0.43	1.03 ± 0.26	5.01 ± 1.26*	1.27 ± 0.26‡
SREBP-1c	0.62 ± 0.07	0.56 ± 0.07	1.12 ± 0.27*	0.63 ± 0.08‡
SREBP-2	0.66 ± 0.11	0.58 ± 0.18	0.45 ± 0.09	0.35 ± 0.08
PPAR-α	0.36 ± 0.17	0.23 ± 0.14	0.26 ± 0.11	0.31 ± 0.04
PPAR-γ	0.51 ± 0.07	0.98 ± 0.31#	1.35 ± 0.12*	2.31 ± 0.34*‡
LXR-α	0.76 ± 0.11	0.70 ± 0.13	1.09 ± 0.14†	0.77 ± 0.11§
LXR-β	0.71 ± 0.08	0.66 ± 0.07	0.83 ± 0.13	0.72 ± 0.09
ACC	0.69 ± 0.10	0.64 ± 0.12	0.62 ± 0.15	0.63 ± 0.03
FAS	0.79 ± 0.07	0.80 ± 0.07	1.03 ± 0.08*	0.89 ± 0.03#
ACO	1.00 ± 0.04	0.93 ± 0.24	2.31 ± 0.79*	1.65 ± 0.58
CYP2E1	0.95 ± 0.10	0.86 ± 0.09	1.57 ± 0.38*	1.08 ± 0.18‡
MTTP	1.09 ± 0.15	0.93 ± 0.25	1.13 ± 0.39	0.93 ± 0.28
HMG-CoA red.	1.29 ± 0.13	1.16 ± 0.13	0.79 ± 0.04*	0.75 ± 0.06*
CHOP	1.15 ± 0.35	1.09 ± 0.44	4.59 ± 0.68*	3.66 ± 0.50*§
SR-A1	0.38 ± 0.06	0.39 ± 0.14	2.02 ± 0.18*	1.04 ± 0.06*‡
CD36	0.35 ± 0.08	0.37 ± 0.09	1.78 ± 0.63*	0.49 ± 0.19‡
TLR-2	0.94 ± 0.07	0.71 ± 0.24	3.06 ± 0.50*	2.09 ± 0.54*‡
TLR-4	0.99 ± 0.25	0.72 ± 0.20	3.75 ± 1.56*	2.14 ± 1.04#
RAGE	0.62 ± 0.07	0.56 ± 0.07	1.12 ± 0.27*	0.63 ± 0.08‡
galectin-3	0.21 ± 0.11	ND	2.10 ± 0.21*	ND

CTGF increased significantly only in *Lgals3*$^{+/+}$ animals, whereas content of α-SMA-positive cells and *collagen I* and *TGF-β* mRNA levels were up-regulated in both genotypes, though significantly more in *Lgals3*$^{+/+}$ vs. *Lgals3*$^{-/-}$ mice (Fig. 3D–F and Table 2).

Liver lipid metabolism

PPAR-γ mRNA expression was higher in *Lgals3*$^{-/-}$ vs. *Lgals3*$^{+/+}$ animals fed a NFD. Upon HFD, gene expression for *SREBP-1*, *LXRα*, *FAS*, *ACO*, and *CYP2E1* increased significantly only in *Lgals3*$^{+/+}$ mice, whereas transcripts for *PPAR-γ* increased and those of *HMG-CoA* reductase decreased significantly in both genotypes, with higher increments in *PPAR-γ* in *Lgals3*$^{+/+}$ vs. *Lgals3*$^{-/-}$ mice (Table 2).

Lipoxidation products and oxidative and ER stress

As previously shown [24,25], circulating ALE/AGE levels in mice assessed for NASH were markedly increased in HFD-fed animals, with significantly higher values in *Lgals3*$^{-/-}$ than in *Lgals3*$^{+/+}$ mice (Table 1). A diffuse liver positivity for both HNE adducts and CML was observed in HFD-fed mice, though it was significantly higher in *Lgals3*$^{+/+}$ vs. *Lgals3*$^{-/-}$ animals (Fig. 4). *CHOP* mRNA levels also increased significantly more in *Lgals3*$^{+/+}$ vs. *Lgals3*$^{-/-}$ mice (Table 2).

ALE/AGE-receptor expression

RAGE and CD36 protein content and mRNA levels increased significantly only in *Lgals3*$^{+/+}$ mice fed a HFD, with immunoreactiv-

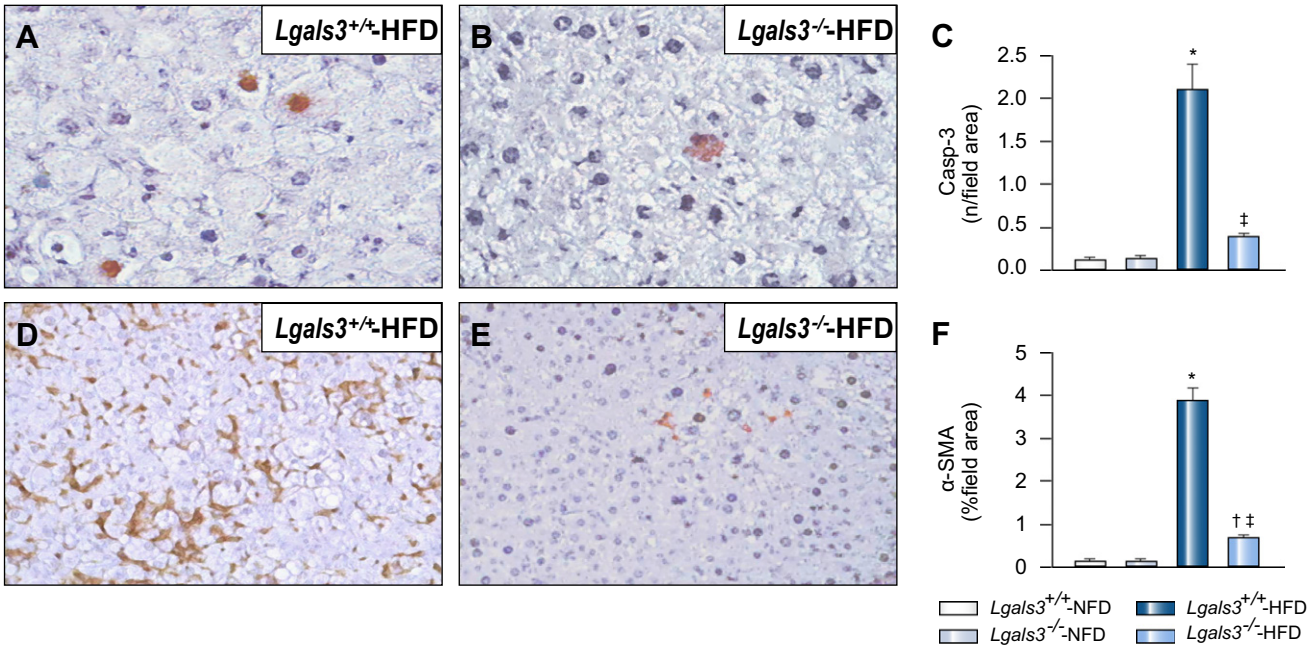

Fig. 3. Apoptosis and HSC myofibroblast differentiation. Representative immunohistochemistry of liver active caspase-3 (A-C), original magnification 250×), and α-SMA (D–F), original magnification 400×) in HFD-fed *Lgals3*$^{+/+}$ and *Lgals3*$^{-/-}$ mice; and quantification in NFD- and HFD-fed *Lgals3*$^{+/+}$ and *Lgals3*$^{-/-}$ mice (mean ± SD; $n = 4$ per group). $^{*}p$ <0.001 or $^{\dagger}p$ <0.01 vs. NFD-fed mice; $^{\ddagger}p$ <0.001 vs. *Lgals3*$^{+/+}$ mice.

ity for RAGE involving inflammatory cells, especially in the portal area, and some ballooned hepatocytes, and that for CD36 remaining confined to sinusoidal endothelial cells (Fig. 5 and Table 2). *SR-A1* and *TLR-2* were up-regulated in mice fed a HFD, with significantly higher increments in *Lgals3*$^{+/+}$ vs. *Lgals3*$^{-/-}$ mice, whereas *TLR-4* mRNA levels increased significantly only in *Lgals3*$^{+/+}$ animals (Table 2). Galectin-3 protein expression, which was limited to Kupffer cells and biliary ducts in NFD-fed *Lgals3*$^{+/+}$ mice, increased significantly in HFD-fed animals also showing positivity for hepatocytes (Supplemental Fig. 1M–O and Table 2).

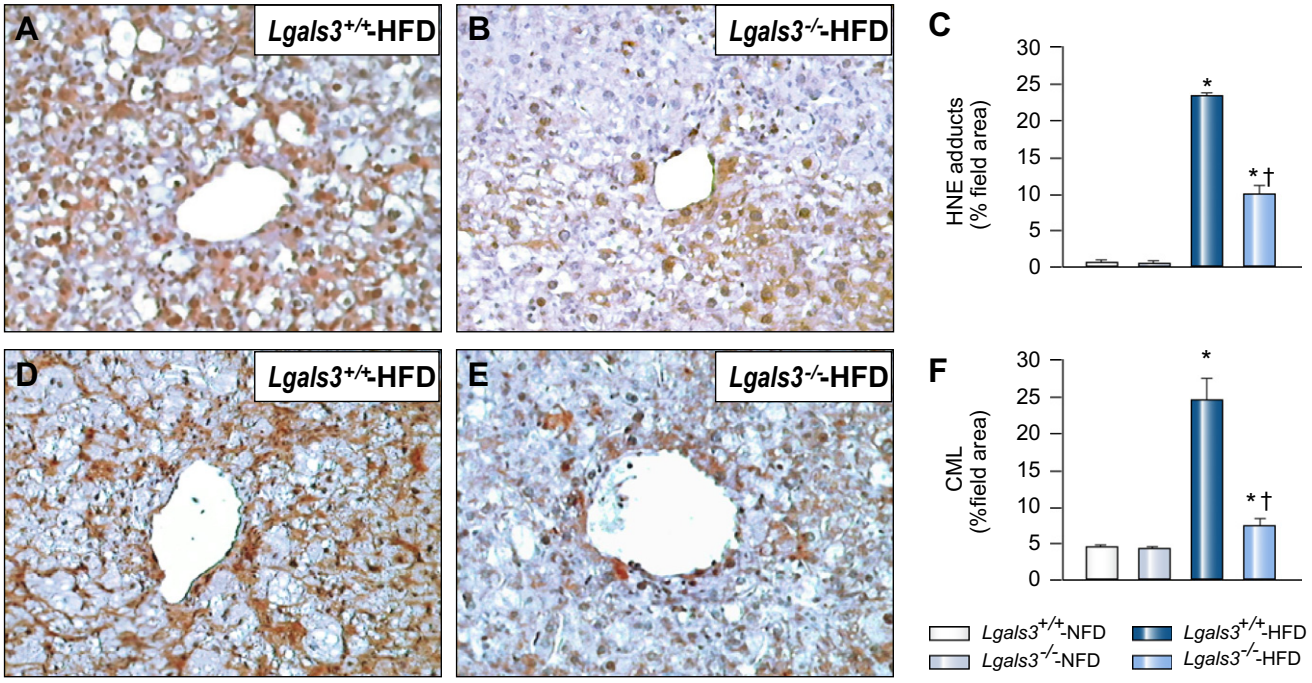

Fig. 4. ALE content. Representative immunohistochemistry (original magnification 250×) of liver HNE adducts (A–C) and CML (D–F) in HFD-fed *Lgals3*$^{+/+}$ and *Lgals3*$^{-/-}$ mice; and quantification in NFD- and HFD-fed *Lgals3*$^{+/+}$ and *Lgals3*$^{-/-}$ mice (mean ± SD; $n = 4$ per group). $^{*}p$ <0.001 vs. NFD-fed mice; $^{\dagger}p$ <0.001 vs. *Lgals3*$^{+/+}$ mice.

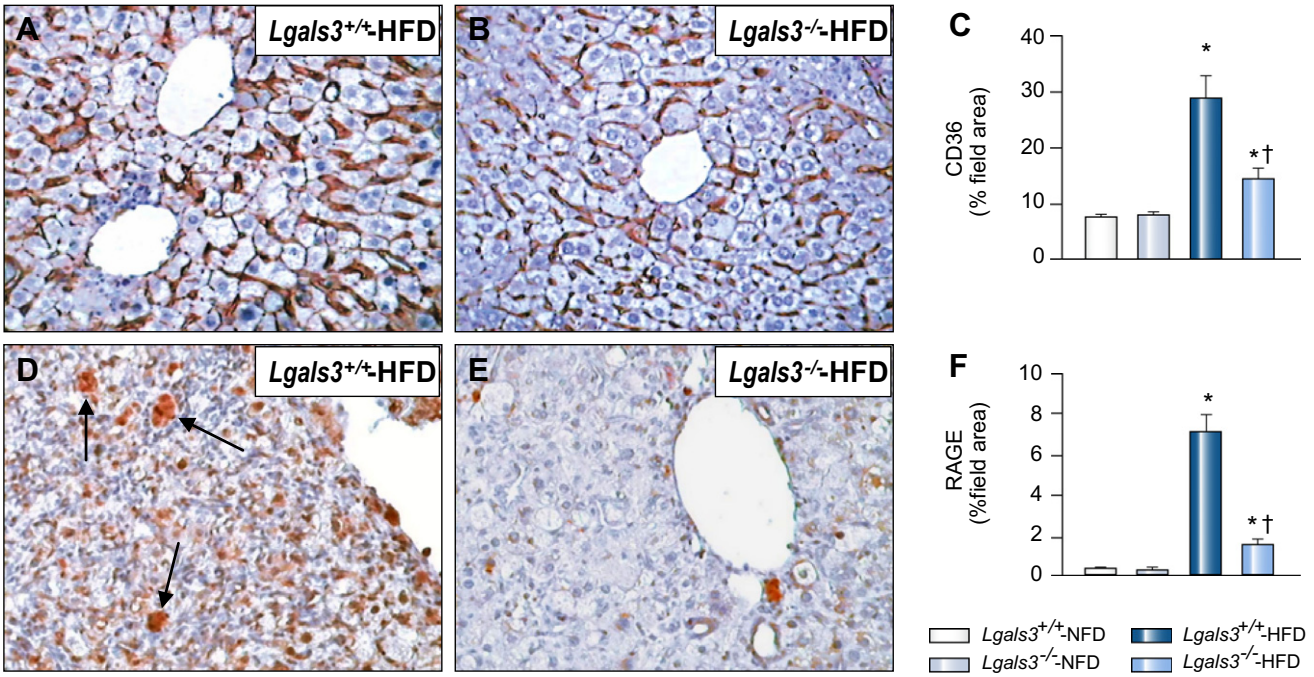

Fig. 5. ALE/AGE-receptors. Representative immunohistochemistry (original magnification 250×) of liver CD36 (A–C) and RAGE (D–F); = RAGE-positive ballooned hepatocytes) in HFD-fed *Lgals3*$^{+/+}$ and *Lgals3*$^{-/-}$ mice; and quantification in NFD- and HFD-fed *Lgals3*$^{+/+}$ and *Lgals3*$^{-/-}$ mice (mean ± SD; $n = 4$ per group). *p <0.001 vs. NFD-fed mice; †p <0.001 vs. *Lgals3*$^{+/+}$ mice.

Insulin signalling

Insulin-stimulated Akt phosphorylation was decreased in HFD- vs. NFD-fed mice, and the extent of reduction was significantly higher in *Lgals3*$^{+/+}$ vs. *Lgals3*$^{-/-}$ mice in liver, but not in muscle (Supplemental Fig. 2).

ALE/AGE uptake by LECs

Galectin-3 silencing (70% reduction) was associated with decreased *CD36*, but not *RAGE* gene expression. Upon challenging with CML-HSA, CML-induced up-regulation of *CD36* and *RAGE* mRNA levels were reduced by *galectin-3* silencing, which also significantly decreased CML uptake by LECs, as evidenced by the reduced and increased CML levels in monolayers and conditioned media, respectively (Fig. 6).

Discussion

Galectin-3-deficient mice showed complete prevention or marked attenuation of NASH induced by an atherogenic diet, consistent with a previous report showing that galectin-3 disruption blocks matrix production in both HSC cultures and in the model of CCl_4-induced cirrhosis [22]. In this earlier study, HSC-driven fibrosis was markedly attenuated, whereas upstream events including liver inflammation/injury and TGF-β expression were unchanged, thus pointing to a primary role for galectin-3 in TGF-β-mediated myofibroblast activation. Here, we provide the first evidence that galectin-3 ablation also influences the earlier steps of NASH, i.e. steatosis, hepatocyte injury, and inflammation. In fact, NASH prevention/attenuation was associated not only with inhibition of HSC-driven fibrosis but also with reduction of (a) infiltration of inflammatory cells and pro-inflammatory pattern of cytokines and transcription factors, (b) ER stress and hepatocyte apoptosis; and (c) up-regulation of TGF-β and CTGF. Both Th1/M1 and Th2/M2 inflammatory responses, which drive hepatocyte damage and fibrosis, respectively [7], were down-regulated in galectin-3-deficient animals.

Several lines of evidence indicate that, among the multiple actions of galectin-3, loss of ALE/AGE receptor function is implicated in the prevention of experimental NASH and suggest that galectin-3 is the main scavenger receptor involved in the hepatic ALE/AGE uptake, i.e.: HFD-fed mice are characterized by increased RCS and ALE/AGE generation from lipid precursors, and ablation of the galectin-3 gene resulted in marked reduction of ALE/AGE accumulation within the liver and increased serum levels of these compounds, pointing to a decreased ALE/AGE clearance. The other AGE/ALE receptors, including SR-A and CD36, were not up-regulated in galectin-3-deficient mice, and this lack of compensation may have further reduced the uptake of ALEs/AGEs. This was confirmed by the reduced CML uptake induced by *galectin-3* silencing in LECs, at variance with previous reports concerning SR-A [16] and CD36 [18].

Hepatic fat accumulation and synthesis were also lower in galectin-3-deficient than in galectin-3-expressing animals, despite similar increases in circulating lipids. This may be attributed to the slightly lower degree of insulin resistance, though it might also be secondary to the reduced extent of liver injury, since the cause-effect relationship between steatosis and insulin resistance is bidirectional [2]. This view is supported by the non-obese phenotype and the nonsignificant increase of free FAs in mice fed an atherogenic diet, suggesting that, in this model, the role of adipose tissue in driving insulin resistance and liver disease is less important, and by the lower impairment of Akt phosphorylation in liver, but not in muscle, in galectin-3-deficient vs.

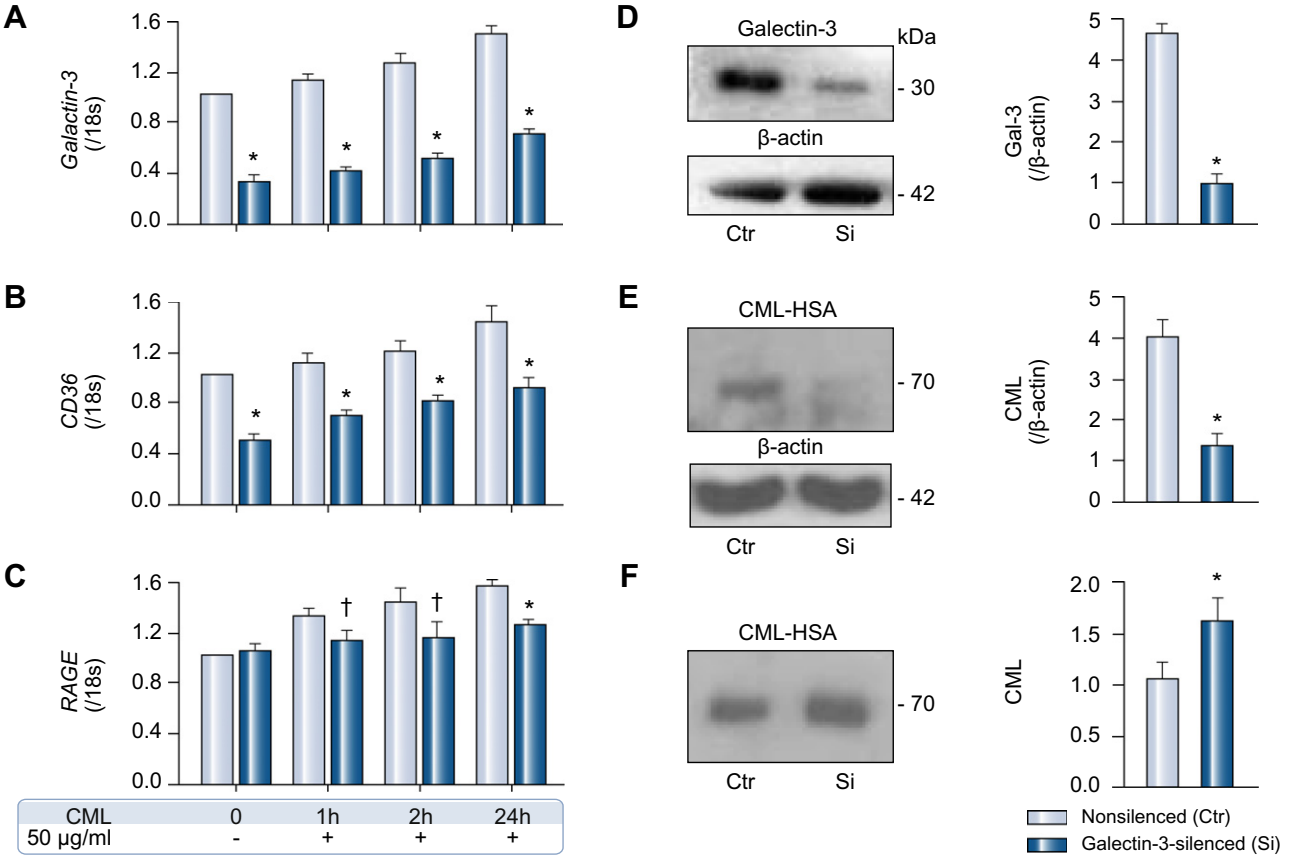

Fig. 6. Galectin-3 silencing in LECs. *Galectin-3*, *CD36*, and *RAGE* mRNA levels in galectin-3-silenced and nonsilenced LECs probed with CML-HSA (A–C); representative Western blots and quantification of galectin-3 protein in cell extracts (D) and CML content in cell extracts (E) and conditioned media (F) from galectin-3-silenced and nonsilenced LECs incubated with CML-HSA for 5 h (optical density; mean ± SD; $n = 3$). $^{*}p < 0.001$ or $^{\dagger}p < 0.01$ vs. nonsilenced LECs.

wild type animals. Reduced FA uptake due to lack of up-regulation of CD36, which serves as an FA translocase, may have contributed to attenuated steatosis, and the blunted up-regulation of FA oxidation associated with decreased fat deposition may have further decreased ALE/AGE accumulation by reducing ROS generation driving lipid peroxidation.

These data, as well as those by Henderson et al. [22], are in contrast with the report of spontaneous NAFLD/NASH occurring with aging in galectin-3-deficient mice [23]. We have no obvious explanation for this discrepancy. In fact, we have followed galectin-3-deficient mice of both sexes for up to 24 months and detected more marked age-related renal changes [28], but no liver disease.

At variance with the liver, in the aorta and kidney of galectin-3-deficient mice fed an atherogenic diet, ALEs/AGEs content was increased, consistent with circulating levels, and other receptors such as RAGE, TLRs, and SRs were up-regulated [24,25]. Moreover, according to the major role of ALEs/AGEs in diet-induced atherosclerosis and renal disease, both these conditions were markedly accelerated [24,25]. Deletion of the *galectin-3* gene also aggravated glomerular injury caused by diabetes [29], CML injection [26], and aging [28], all conditions characterized by increased AGE/ALE levels. Taken together, these data suggest that, in mice lacking galectin-3, impaired AGE/ALE removal by the liver causes increased circulating levels of these compounds and enhanced uptake by vascular and renal tissues via RAGE and other receptors, which trigger pro-oxidant and pro-inflammatory pathways leading to injury in these extra-hepatic tissues. Thus, tissue discrepancies in the consequences of galectin-3 ablation seem to reflect tissue differences in the function of the ALE/AGE receptor system, which, in the liver, is mainly implicated in ALE/AGE removal/detoxification. This interpretation is in keeping with the view that the role of galectin-3 *in vivo* is dependent on the type of injurious stimulus and the context of organ damage [30].

In conclusion, galectin-3 ablation prevents the development of NASH induced by an atherogenic diet by inhibiting not only HSC myofibroblast transdifferentiation and fibrosis but also oxidant-dependent tissue inflammation and hepatocyte injury. It also reduced up-regulation of lipid synthesis and oxidation, causing less fat deposition (and possibly insulin resistance) and oxidative stress (with reduced ALE generation), respectively. These effects can be attributed to a reduced LEC uptake and hepatic ALE/AGE accumulation, which suggests that galectin-3 is a major scavenger receptor involved in ALE/AGE uptake by the liver, a central mechanism for clearing these compounds from the circulation and preventing deposition in extra-hepatic tissues.

Financial support

This work was supported by grants from the European Foundation for the Study of Diabetes/Juvenile Diabetes Foundation International/Novo Nordisk, the Telethon Foundation, the Ministry of

University and Research of Italy, and the Diabetes, Endocrinology and Metabolism Foundation, Rome, Italy.

Conflict of interest

The authors who have taken part in this study declared that they do not have anything to disclose regarding funding or conflict of interest with respect to this manuscript.

Supplementary data

Supplementary data associated with this article can be found, in the online version, at doi:10.1016/j.jhep.2010.09.020.

References

[1] Erickson SK. Nonalcoholic fatty liver disease. J Lipid Res 2009;50:S412–416.
[2] Marchesini G, Bugianesi E, Forlani G, Cerrelli F, Lenzi M, Manini R, et al. Nonalcoholic fatty liver, steatohepatitis, and the metabolic syndrome. Hepatology 2003;37:917–923.
[3] Bradbury MW, Berk PD. Lipid metabolism in hepatic steatosis. Clin Liver Dis 2004;8:639–671.
[4] Anstee QM, Goldin RD. Mouse models in non-alcoholic fatty liver disease and steatohepatitis research. Int J Exp Pathol 2006;87:1–16.
[5] Maher JJ, Leon P, Ryan JC. Beyond insulin resistance. Innate immunity in nonalcoholic steatohepatitis. Hepatology 2008;48:670–678.
[6] Koteish A, Diehl AM. Animal models of steatosis. Semin Liver Dis 2001;21:89–104.
[7] Choi S, Diehl AM. Role of inflammation in nonalcoholic steatohepatitis. Curr Opin Gastroenterol 2005;21:702–707.
[8] Negre-Salvayre A, Coatrieux C, Ingueneau C, Salvayre R. Advanced lipid peroxidation end products in oxidative damage to proteins. Potential role in diseases and therapeutic prospects for the inhibitors. Br. J. Pharmacol. 2008;153:6–20.
[9] George J, Pera N, Phung N, Leclercq I, Yun Hou J, Farrell G. Lipid peroxidation, stellate cell activation and hepatic fibrogenesis in a rat model of chronic steatohepatitis. J Hepatol 2003;39:756–764.
[10] Sěbeková K, Kupčová V, Schinzel R, Heidland A. Markedly elevated levels of plasma advanced glycation end products in patients with liver cirrhosis–amelioration by liver transplantation. J Hepatol 2002;36:66–71.
[11] Smedsrød B, Melkko J, Araki N, Sano H, Horiuchi S. Advanced glycation end products are eliminated by scavenger-receptor-mediated endocytosis in hepatic sinusoidal Kupffer and endothelial cells. Biochem J 1997;322:567–573.
[12] Moore KJ. Freeman MW: Scavenger receptors in atherosclerosis: beyond lipid uptake. Arterioscler Thromb Vasc Biol 2006;26:1702–1711.
[13] Hansen B, Svistounov D, Olsen R, Nagai R, Horiuchi S, Smedsrød B. Advanced glycation end products impair the scavenger function of rat hepatic sinusoidal endothelial cells. Diabetologia 2002;45:1379–1388.
[14] Targher G, Marra F, Marchesini G. Increased risk of cardiovascular disease in non-alcoholic fatty liver disease: causal effect or epiphenomenon? Diabetologia 2008;51:1947–1953.
[15] Chou MY, Hartvigsen K, Hansen LF, Fogelstrand L, Shaw PX, Boullier A, et al. Oxidation-specific epitopes are important targets of innate immunity. J Intern Med 2008;263:479–488.
[16] Matsumoto K, Sano H, Nagai R, Suzuki H, Kodama T, Yoshida M, et al. Endocytic uptake of advanced glycation end products by mouse liver sinusoidal cells is mediated by a scavenger receptor distinct from the macrophage scavenger receptor class A. Biochem J 2000;352:233–240.
[17] Kunjathoor VV, Febbraio M, Podrez EA, Moore KJ, Andersson L, Koehn S, et al. Scavenger receptors class A-I/II and CD36 are the principal receptors responsible for the uptake of modified low density lipoprotein leading to lipid loading in macrophages. J Biol Chem 2002;277:49982–49988.
[18] Nakajou K, Horiuchi S, Sakai M, Hirata K, Tanaka M, Takeya M, et al. CD36 is not involved in scavenger receptor–mediated endocytic uptake of glycolaldehyde- and methylglyoxal-modified proteins by liver endothelial cells. J Biochem 2005;137:607–616.
[19] Butscheid M, Hauptvogel P, Fritz P, Klotz U, Alscher D. Hepatic expression of Galectin-3 and RAGE in patients with liver disease. J Clin Pathol 2007;60:415–418.
[20] Xia J-R, Liu N-F, Zhu N-X. Specific siRNA targeting the receptor for advanced glycation end products inhibits experimental hepatic fibrosis in rats. Int J Mol Sci 2008;9:638–661.
[21] Fehrenbach H, Weiskirchen R, Kasper M, Gressner AM. Up-regulated expression of the receptor for advanced glycation end products in cultured rat hepatic stellate cells during transdifferentiation to myofibroblasts. Hepatology 2001;34:943–952.
[22] Henderson NC, Mackinnon AC, Farnworth SL, Poirier F, Russo FP, Iredale JP, et al. Galectin-3 regulates myofibroblast activation and hepatic fibrosis. Proc Natl Acad Sci USA 2006;103:5060–5065.
[23] Nomoto K, Tsuneyama K, Abdel Aziz HO, Takahashi H, Murai Y, Cui Z-G, et al. Disrupted galectin-3 causes non-alcoholic fatty liver disease in male mice. J Pathol 2006;210:469–477.
[24] Iacobini C, Menini S, Ricci C, Scipioni A, Sansoni V, Cordone S, et al. Accelerated lipid-induced atherogenesis in galectin-3-deficient mice. role of lipoxidation via receptor-mediated mechanisms. Arterioscler Thromb Vasc Biol 2009;29:831–836.
[25] Iacobini C, Menini S, Ricci C, Scipioni A, Sansoni V, Mazzitelli G, et al. Advanced lipoxidation end-products mediate lipid-induced glomerular injury: role of receptor-mediated mechanisms. J Pathol 2009;218:360–369.
[26] Iacobini C, Menini S, Oddi G, Ricci C, Amadio L, Pricci F, et al. Galectin-3/AGE-receptor 3 knockout mice show accelerated AGE-induced glomerular injury. Evidence for a protective role of galectin-3 as an AGE-receptor. FASEB J 2004;18:1773–1775.
[27] Neuschwander-Tetri BA, Caldwell SH. Nonalcoholic steatohepatitis: summary of an AASLD Single Topic Conference. Hepatology 2003;37:1202–1219.
[28] Iacobini C, Oddi G, Menini S, Amadio L, Ricci C, Barsotti P, et al. Development of age-dependent glomerular lesions in galectin-3/AGE-receptor-3 knockout and wild type mice. Am J Physiol 2005;289:F611–F621.
[29] Pugliese G, Pricci F, Iacobini C, Leto G, Amadio L, Barsotti P, et al. Accelerated diabetic glomerulopathy in galectin-3/AGE-receptor-3 knockout mice. FASEB J 2001;15:2471–2479.
[30] Henderson NC, Sethi T. The regulation of inflammation by galectin-3. Immunol Rev 2009;230:160–171.